Available online at www.sciencedirect.com
SCIENCE DIRECT
Journal of Molecular Catalysis A: Chemical 247 (2006) 248–252
JOURNAL OF MOLECULAR CATALYSIS A: CHEMICAL
www.elsevier.com/locate/molcata

EMR characterisation of $La_{1.8}M_{0.2}CuO_4$ and $La_{0.9}M_{0.1}CoO_3$ (M = Pr, Sm, Tb) catalysts for methane flameless combustion

C. Oliva [a,*], S. Cappelli [a], A. Kryukov [b], G.L. Chiarello [a], A.V. Vishniakov [b], L. Forni [a]

[a] *Dipartimento di Chimica Fisica ed Elettrochimica, Università di Milano, via C. Golgi, 19, 20133 Milano, Italy*
[b] *D.I. Mendeleev University of Chemical Technology of Russia, Moscow, Russia*

Received 13 October 2005; received in revised form 29 November 2005; accepted 30 November 2005
Available online 6 January 2006

Abstract

A few perovskite-like and fluorite-like samples in which M = Pr, Sm or Tb substitutes for La have been characterised by electron magnetic resonance (EMR) spectroscopy and other techniques. Ferromagnetic (FM) systems form with the fresh biphasic sample with M = Sm only, but not after recalcination, when it becomes monophasic. These systems could be formed of Magnetic Bound Polarons due to the thermally excited $J = 1$ Sm^{2+} ions present as impurity in the former case. FM systems form also with the M = Tb sample, but only after catalytic use. In this case FM systems could be composed of Tb^{4+} ions forming during sample re-oxidation. All these EMR observations have been correlated with the catalytic performance of these samples.

Keywords: Partially substituted perovskites; Partially substituted fluorites; EPR; Ferromagnetic resonance; Magnetic Bound Polarons; Catalytic methane combustion

1. Introduction

Catalytic combustion has been proposed as an effective method for oxidation of fuel/air lean mixtures with low emission of NO_x, CO and unburnt hydrocarbons [1,2], due to the lower combustion temperature in comparison with usual combustion [1,3].

Noble metals based catalysts are the most active, especially at low temperature, but they are expensive and poorly stable because of sintering and volatilisation of the active phase. On the other hand, transition metal oxides are cheaper, but usually less active [1,2,4]. Much attention has been paid to perovskite-type oxides of general formula ABO_3 as catalysts for total oxidation of hydrocarbons, because of their high activity and thermal stability [1,2,5]. A lot of perovskite-like $La_{0.9}M_{0.1}CoO_3$ compositions have been recently tested and that with M = Ce resulted the most active. Indeed, non-stoichiometric compounds including d and f M elements with changeable oxidation state can contain weakly bound oxygen and possess a high oxygen storage capacity. However, the role played by the oxidation state of M is still not completely clear.

All rare-earth elements share a common (3+) ground oxidation state and only cerium, terbium and praseodymium can share the oxidation state 4+, while samarium can be in the oxidation state 2+. The highest terbium and praseodymium oxides are unstable in comparison with CeO_2 and normally exist as Pr_7O_{12} (Pr_6O_{11}) and Tb_7O_{12}, i.e. they include rare elements in two oxidation states 3+ and 4+ in 2:3 ratio. At high temperature higher oxides decompose to sesquioxides losing oxygen. It means that the oxygen storage capacity of these oxides is higher than for ceria. In the present investigation we analysed some $La_{0.9}M_{0.1}CoO_3$ perovskite-like catalysts and $La_{2-x}M_xCuO_4$ fluorite-like catalysts (M = Pr, Sm, Tb) aiming at a better understanding of the role played by the oxidation state of M and the effect of preparation procedure on activity of these solids in the catalytic flameless combustion (CFC) of methane.

2. Experimental

2.1. Catalysts preparation

Traditionally, these materials were synthesised through several cycles of calcination-milling (CM), leading to a ther-

* Corresponding author. Tel.: +39 02 50314270; fax: +39 02 50314300.
E-mail address: cesare.oliva@unimi.it (C. Oliva).

1381-1169/$ – see front matter © 2005 Elsevier B.V. All rights reserved.
doi:10.1016/j.molcata.2005.11.056

mally resistant catalyst, but with a too low (1–2 m^2/g) specific surface area (SSA) and hence with low activity [1]. The sol–gel (SG) procedure [6] allows to obtain higher SSA (ca. 30–40 m^2/g), but the final calcination temperature being relatively low (600–700 °C), the material is thermally poorly resistant. Both these properties, thermal stability and high SSA, can be achieved by preparing the material in very small particles, calcined at very high temperature. The preparation method based on flame-hydrolysis of an aqueous solution of the precursors salts [7] allows to produce materials with very good thermal stability and SSA of about 15–20 m^2/g, but the productivity of the method is quite low (less than 0.03 g/h) [8]. An alternative flame-based method (flame-spray pyrolysis—FSP) consists in the combustion of an organic precursor solution and permits to obtain nanoparticles with SSA higher than 50 m^2/g (sometimes even more than 100 m^2/g) in quantity of 3–4 g/h [9].

All the samples examined in the present investigation were prepared by the FSP method [9]. Briefly, the precursor solution of metal acetates in combustible organic solvent (20 cm^3 of propionic acid + 40 cm^3 of 2-ethyl-hexanoic acid) is fed by means of a syringe pump through a capillary tube ending in the centre of the main nozzle of the burner. Oxygen, needed for both dispersion and combustion of the solution, is fed to the burner through the free space around the capillary tube. Organic solution and oxygen form a vertical flame, supported by a crown of small CH_4/O_2 flamelets. The nanosize particles produced in the flame are collected by means of a 10 kV electrostatic precipitator.

2.2. Catalysts characterisation

SSA and porosity were determined by adsorption–desorption of N_2 at liquid nitrogen temperature, by means of a Micromeritics ASAP 2010 instrument. XRD analysis was carried out with a Philips PW1820 powder diffractometer, using the Ni-filtered Cu Kα radiation (λ = 0.15418 nm). The shape and size of the particles were determined by means of a Leica LEO 1430 scanning electron microscope (SEM). Electron paramagnetic resonance (EPR) analysis was carried out with a Bruker ELEXSYS EPR-ENDOR instrument on loose-packed powdered samples loaded in cylindric quartz tubes (WILMAD, 081707-SQ250M, internal diameter 3 mm, external diameter 4 mm). The same amount of powder was always loaded in the tube in the different experiments. In few cases, the sample was mounted at an arbitrary orientation on a goniometer and then the EPR spectrum was collected at two different sample orientations, differing 90° from each other, and preventing any shift of the sample as a whole in the external magnetic field during the field scanning. In the case of EPR measurements performed with both increasing and decreasing magnetic field, the former measurement was always carried out before the latter. Then the sample was kept 15 min in a 4000 G intense magnetic field, before recording the electron magnetic resonance (EMR) pattern with magnetic field decreasing from 4000 down to 0 G.

3. Results

3.1. Catalysts characterisation

All the present lanthanum cobaltites possessed a SSA in the 50–60 m^2/g range. Lanthanum cuprates had a little lower SSA (40–45 m^2/g). SEM analysis showed that all the samples were made of uniform spherical particles, 20–40 nm in size, clustered in agglomerates of larger size.

The XRD patterns of $La_{1.8}M_{0.2}CuO_4$ samples were very similar to each other, independently of the nature of M. The same was for $La_{0.9}M_{0.1}CoO_3$. Fig. 1a reports the case of cuprate with M = Sm. Arrows indicate the reflections due to a La_2O_3 phase, present in all of the cuprate samples. These reflections disappeared only after recalcination at 800 °C for 1.5 h. A different situation was observed with $La_{0.9}M_{0.1}CoO_3$ samples. Indeed, only the perovskite phase was present in all of them (see, e.g. Fig. 1b for M = Sm).

3.2. EPR spectra

3.2.1. $La_{1.8}M_{0.2}CuO_4$ (M= Pr, Sm, Tb)

All the cuprate samples showed the Cu^{2+} EPR spectrum typical of magnetically diluted Cu^{2+} systems (see inset of Fig. 2). No significant difference can be noticed among them, concerning this pattern.

A further magnetic resonance feature (FM in Fig. 2) added at lower magnetic field with $La_{1.8}Sm_{0.2}CuO_4$ only. FM phase was characterised by an intensity strongly increasing with temperature in the 120 K < T < 298 K range. All the spectra have been collected with magnetic field intensity increasing from 0 up to 8000 G at the rate of 200 G s^{-1}. After that scanning the spectrum of $La_{1.8}Sm_{0.2}CuO_4$ was collected, at room temperature, also with the magnetic field decreasing from 4000 to 0 G. This pattern is reported in Fig. 3 and compared to that recorded with increasing magnetic field. We can observe that the former is more intense in the low field (LF) region. The spectral shape of FM depended also on the orientation of the sample inside the EPR cavity. For example, the patterns of Fig. 4 were collected with

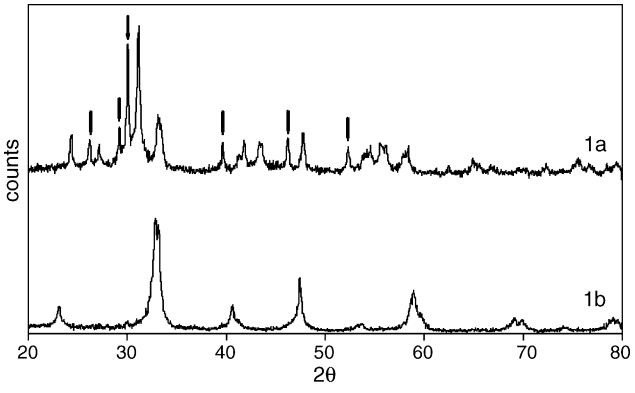

Fig. 1. XRD patterns: $La_{1.8}Sm_{0.2}CuO_4$ (1a) and $La_{0.9}Sm_{0.1}CoO_3$ (1b). Arrows indicate the presence of La_2O_3 phase. The latter disappeared after 1 h sample recalcination at 800 °C.

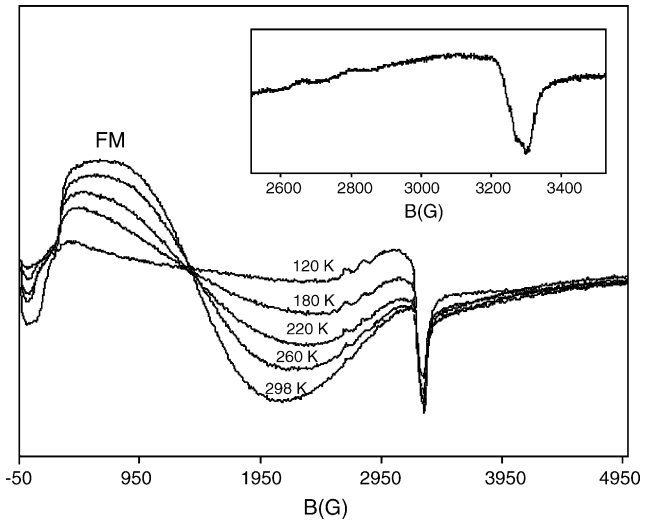

Fig. 2. The temperature dependent EPR spectrum of fresh $La_{1.8}Sm_{0.2}CuO_4$. Inset: room temperature EPR spectrum of fresh $La_{1.8}Sm_{0.2}CuO_4$—detail corresponding to $g_{//} = 2.35$; $g_{\perp} = 2.06$; $A_{//} = 144$ G.

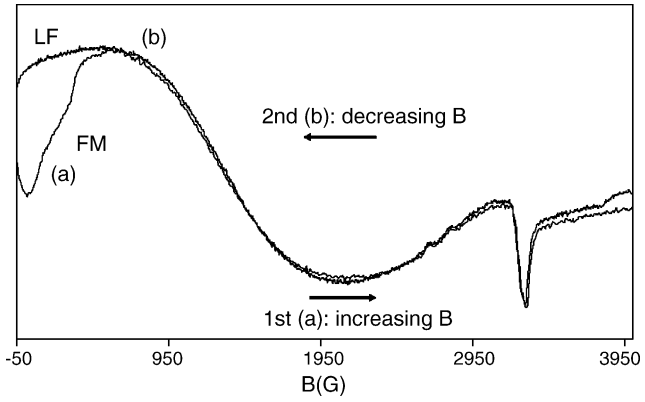

Fig. 3. Room temperature EPR spectrum of fresh $La_{1.8}Sm_{0.2}CuO_4$ with increasing and, then, with decreasing magnetic field.

increasing magnetic field at two sample orientations, differing 90° from each other.

The FM pattern disappeared after recalcining this sample at 800 °C for 1.5 h. By contrast, a very broad and intense FM band

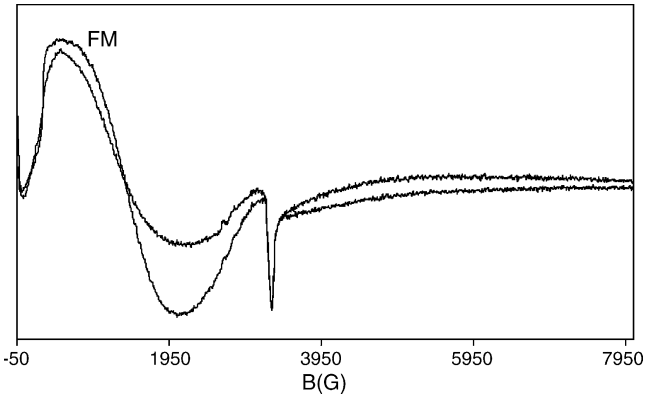

Fig. 4. Room temperature EPR spectra of fresh $La_{1.8}Sm_{0.2}CuO_4$. Sample at two different orientations differing by 90°.

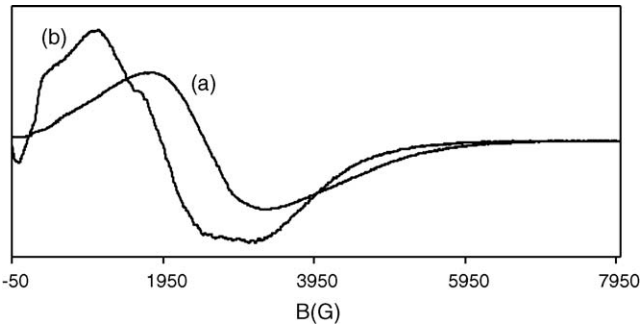

Fig. 5. Room temperature EPR spectra of $La_{1.8}M_{0.2}CuO_4$ after use as catalysts for the CFC of methane: (a) M = Sm and (b) M = Tb.

was observed when using this cuprate sample or that with M = Tb as catalyst for the CFC of methane (Fig. 5), while traces of the Cu^{2+} EPR pattern were then observable only at $T < 120$ K. However, with these two used catalysts, the spectral intensity of the FM band showed a different trend with increasing temperature (Fig. 6). By contrast, no FM band at all appeared with the Pr-containing cuprate catalyst after catalytic use.

3.2.2. $La_{0.9}M_{0.1}CoO_3$ (M = Pr, Sm, Tb)

At room temperature, no EMR spectra were observed with these samples, when fresh. An intense low-field FM feature was observed with the M = Sm sample only, but uniquely after its use as catalysts for the CFC of methane. A broad band showed also with the M = Tb used catalyst, but this pattern was by far less intense than in the previous case and characterised by $g \cong 2$. By contrast, no EMR spectrum at all was observed with the used M = Pr sample. Hence, with these samples the EMR spectra were recorded at room temperature only.

3.3. Activity tests for the CFC of methane

All the $La_{0.9}M_{0.1}CoO_3$ showed better catalysts than $La_{1.8}M_{0.2}CuO_4$. However, here we discuss in detail only the cases of $La_{1.8}Sm_{0.2}CuO_4$ before and after 1 h recalcination at 800 °C (Figs. 7 and 8) and that of $La_{0.9}Sm_{0.1}CoO_3$ (Fig. 8), which can help the discussion.

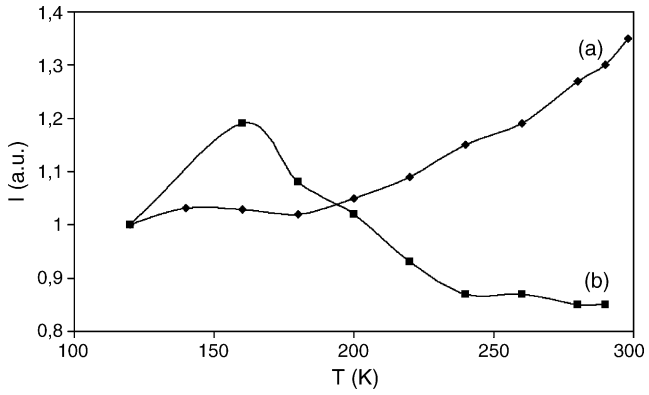

Fig. 6. Spectral intensity (a.u.) of $La_{1.8}M_{0.2}CuO_4$ samples after use for the CFC of methane: (a) M = Sm and (b) M = Tb.

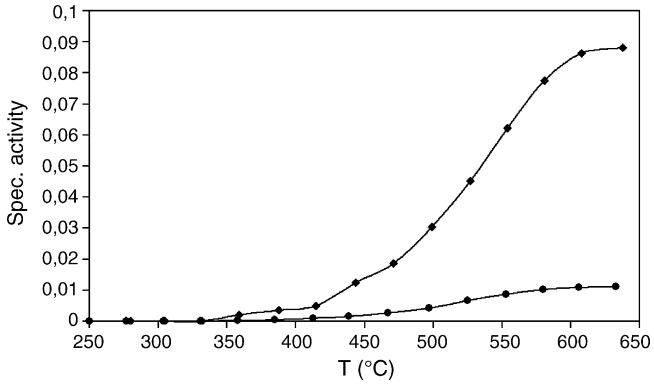

Fig. 7. Activity per unit surface area for the CFC of methane shown by $La_{1.8}Sm_{0.2}CuO_4$ before (●) and after (♦) 1 h recalcination at 800 °C.

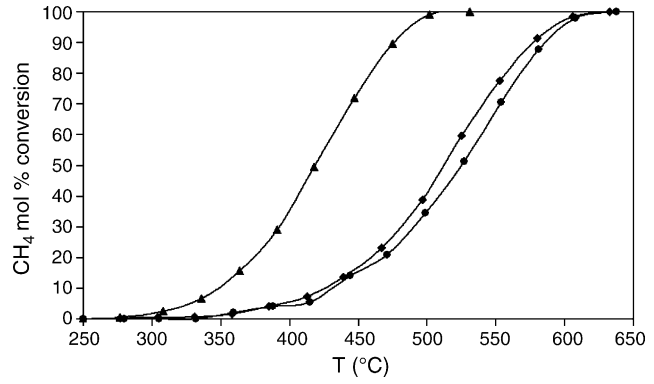

Fig. 8. Activity per unit mass for the CFC of methane: $La_{1.8}Sm_{0.2}CuO_4$ before (●) and after (♦) 1 h recalcination at 800 °C; (▲) $La_{0.9}Sm_{0.1}CoO_3$.

4. Discussion

Cu^{2+} is a regular component of $La_{1.8}M_{0.2}CuO_4$. Therefore, it should be surprising that these systems show the EPR spectrum typical of diluted Cu^{2+}, i.e. with a resolved hyperfine structure instead of displaying a broad single EMR band due to spin–spin coupling among adjacent paramagnetic ions. However, it is well known that, in general, such an intense band is not observed with cuprates. Indeed, adjacent Cu^{2+} ions interact with each other by super-exchange through the O bridge. Therefore, Cu^{2+} should be completely EPR silent in these compounds, with the only exception of those belonging to some defects in Cu-subsystem involving oxygen vacancies or forming isolated paramagnetic entities.

Furthermore, in the present case the poor resolution of the Cu^{2+} EPR spectra does not permit to observe any significant difference between distortions occurring in the Cu^{2+} neighbours of these defects when Pr^{3+}, Sm^{3+} or Tb^{3+} substitute for La^{3+}, though the ionic radius r of these ions is rather different, being $r = 1.09$, 1.04 and 1.00 Å, respectively, and in any case lower than for La^{3+} (1.15 Å).

Pr^{3+}, Sm^{3+} and Tb^{3+} are paramagnetic ions [10]. However, their spin–lattice relaxation rate is generally so high that no EPR spectrum is expected at temperature higher than 20 K. Indeed, only the S-state ($L = 0$; $4f^7$) of Eu^{2+}, Gd^{3+} and Tb^{4+} lanthanide ions can show an EPR spectrum at higher temperature [11,12]. However, no Tb^{4+} can be noticed in our Tb-containing fresh sample, indicating that Tb^{3+} only is present in it. The broad band detected with fresh $La_{1.8}Sm_{0.2}CuO_4$, not attributable to Sm^{3+} ions, undergoes the hysteresis effect of Fig. 3, so that it cannot be attributed to EPR resonance but, instead, to ferromagnetic (FM) resonance (FMR) [13]. This means that FM domains form in this sample, generating an internal field B_i and, therefore, a spectral shift towards lower fields [14]. Furthermore, such systems should not be distributed uniformly throughout the bulk, as suggested by the dependence of the spectrum on the sample orientation (Fig. 4). FM clusters have been reported with Sm-containing perovskites, namely with $Sm_{0.2}Ca_{0.8}Mn_{1-x}Ru_xO_3$ [15], and attributed to the formation of "Bound Magnetic Polarons" (BMP), also indicated as "Ferrons" [16]. These systems should form in the presence of free electrons concentrated enough to form local FM "droplets".

Electron energy decreases with increasing the FM order in the crystal. Therefore, FM "droplets" tend to grow up. Indeed, a high FM order forms in the vicinity of a donor, like Sm^{2+} ions. In fact, XRD patterns of $La_{1.8}M_{0.2}CuO_4$ clearly reveal the presence of a La_2O_3 phase (see, for example, Fig. 1a for M = Sm). Therefore, the following reactions should occur in these samples:

$$10La_{1.8}M_{0.2}CuO_4 \rightarrow 9La_2O_3 + 10CuO + M_2O_3 \quad (1)$$

$$Pr_2{}^{3+}O_3{}^{2-} \rightarrow 2Pr^{2+}O^{2-} + \tfrac{1}{2}O_2 \quad (2)$$

$$Sm_2{}^{3+}O_3{}^{2-} \rightarrow 2Sm^{2+}O^{2-} + \tfrac{1}{2}O_2 \quad (3)$$

$$Tb_2{}^{3+}O_3{}^{2-} + \tfrac{1}{2}O_2 \rightarrow 2Tb^{4+}O_2{}^{2-} \quad (4)$$

No clear evidence of $M_2{}^{3+}O_3$ nor of $M^{2+}O$ phase is evidenced in the XRD pattern, suggesting that these compounds are dispersed or grouped into disordered clusters. Furthermore, Pr^{2+} and Pr^{3+} could not be detected at these temperatures, as above mentioned. Sm^{2+} are diamagnetic ($J = 0$) $4f^6$ ions. However, the energy of the first excited (paramagnetic) $J = 1$ state is less than 300 cm^{-1} higher with this ion, i.e. comparable with the room temperature energy (~200 cm^{-1}), at difference with the other rare-earth ions, with which this difference generally is of some thousands cm^{-1}. This should explain the fact that BMP are observed with the Sm^{3+}-containing cuprate sample only, in which Sm^{2+}-containing clusters should form through reactions (1) and (3). This is also in line with the increase of spectral intensity with increasing temperature. Indeed, higher temperatures favour the excitation from the diamagnetic to the paramagnetic Sm^{2+} state. XRD patterns reveal also that La_2O_3 is no more present in these cuprate samples after their recalcination at 800 °C. Therefore, reactions (1)–(3) cannot occur anymore after such a treatment. On the other hand, also the FM band is then no more detected with M = Sm cuprate. This further supports the attribution of this band to the Sm^{2+} FM clusters, forming only when reaction (3) occurs. Furthermore, no other cuprate, when fresh, reveals FM species, though they all show nearly the same Cu^{2+} EPR pattern. Therefore, the defects generating this spectrum seem neither significantly involved in the formation of Sm^{2+} FM clusters, nor affected by their presence. In addition, also $La_{0.9}Sm_{0.1}CoO_3$ reveals a FM band (though

only after catalytic use), further suggesting that Sm, and not Cu ions, are involved in the formation of FM species.

$La_{1-x}M_xCoO_3$ perovskite-like systems, with M = Ca, Sr, have been widely investigated in literature [17–20]. The substitution of these M^{2+} ions for La^{3+} increased the concentration of Co^{4+} ions, forming a FM order due to double-exchange interactions between Co^{3+} and Co^{4+} ions. At the same time antiferromagnetic (AFM) superexchange was occurring between Co^{3+}–Co^{3+} and Co^{4+}–Co^{4+} ions, strongly competing with FM interactions, so to generate magnetic frustration phenomena. As a consequence, a narrow resonance window in the $g \cong 2$ spectral region was observed at enough high temperature, while at lower temperature, when FM interactions were prevailing, a broader and asymmetric feature was observed at lower field. All these phenomena require the formation of Co^{4+} ions, though also oxygen-based species are perhaps involved [20]. In the present investigation, no $g \cong 2$ line was noticed at high temperature, and only the low-field FM feature due to the ($J = 1$) Sm^{2+} clusters was observed. This suggests that no significant concentration of Co^{4+} is present in these Sm-containing cobaltites. Indeed, the ionisation reaction $Co^{3+} \rightarrow Co^{4+}$ would require (in the ideal gas phase) 4950 J mol^{-1}, very close to $Ca^{2+} \rightarrow Ca^{3+}$ (4912 J mol^{-1}) and $Sr^{2+} \rightarrow Sr^{3+}$ (4138 J mol^{-1}). Therefore, the substitution of Ca and Sr for La in the perovskitic lattice is energetically competitive with the oxidation of Co^{3+} to Co^{4+}. This is no more the case for the substitution of Sm for La. Indeed, the $Sm^{2+} \rightarrow Sm^{3+}$ reaction requires 2260 J mol^{-1} only, being energetically favoured with respect to the formation of Co^{4+} from Co^{3+}. However, in a disordered system a few Sm^{2+} ions can be close to each other, so that, when thermally excited up to their paramagnetic ($J = 1$) state, they can form FM systems. This would occur, with Sm-containing cobaltite, only after catalytic use, at difference with Sm-containing cuprate. This is in line with the observation that only the former, when fresh, is a monophasic "ordered" solid. Disorder is introduced in its structure only during its use as catalyst.

Different considerations must be done in the case of M = Tb. Indeed, the only EPR-detectable species would be Tb^{4+}, which can form only by sample re-oxidation (reaction (4)), i.e. after catalytic reaction, as observed. However, these species would be different from those noticed with M = Sm. In fact, with Sm-containing samples FM species are favoured at higher temperature only (Fig. 6a), while in the (used) Tb-containing cuprate catalyst the trend of the FM spectral intensity versus temperature indicates a "normal" Curie–Weiss behaviour, possibly with antiferromagnetic coupling at low temperature (Fig. 6b). Reactions (1)–(3) should occur also at low temperature, accounting for the low catalytic performance per unit SSA shown by these (not recalcined) cuprates for the CFC of methane (see, e.g. Fig. 7). In fact, this sample would lose oxygen even at a temperature by far lower than that of methane combustion. The catalytic activity per unit SSA increases markedly with the recalcined samples (Fig. 7), in which M perfectly substitutes for La in the fluorite-like crystal structure, so that oxygen is no more lost at low temperature through reactions (2) and (3). However, though a partial sintering accompanies this recalcination process, causing a decrease of SSA, the catalytic activity per unit mass does not change significantly (Fig. 8) after this treatment, probably because of a counterbalancing effect due to the disappearance of MBP.

The presence of FM with the Sm-containing cobaltite sample only after its use as catalyst, together with the increase of FM intensity after use of Sm-containing and Tb-containing cuprates, indicates that FM is not related to any catalytically active species, but possibly to species whose concentration increases during the catalytic reaction. In fact, the better catalysts ($La_{0.9}Sm_{0.1}CoO_3$ and recalcined $La_{1.8}Sm_{0.2}CuO_4$, upper curves in Figs. 7 and 8) do not reveal any FM species when fresh.

5. Conclusions

Biphasic fluorite-like catalysts may possess high SSA, but their catalytic activity can be lowered by the formation of MBP. Indeed, MBP cause a grouping of electrons, which become less available for the catalytic reaction. Sample recalcination causes a decrease of SSA due to sample sintering, however, counterbalanced by the increase of catalytic activity due to the disappearance of MBP.

Acknowledgment

We are indebted to R. Basosi for useful discussion and suggestions during the laying down of the paper.

References

[1] M.F. Zwinkels, S.G. Järås, P.G. Menon, Catal. Rev. Sci. Eng. 35 (1993) 319.
[2] K. Eguchi, H. Arai, Catal. Today 29 (1996) 379.
[3] H. Arai, M. Machida, Catal. Today 10 (1991) 81.
[4] R. Burch, Catal. Today 35 (1997) 27.
[5] J.G. Mc Carty, H. Wise, Catal. Today 8 (1990) 231.
[6] M.S.G. Baythoun, F.R. Sale, J. Mater. Sci. 17 (1982) 2757.
[7] R.A.M. Giacomuzzi, M. Portinari, I. Rossetti, L. Forni, in: A. Corma, F.V. Melo, S. Mendioroz, J.L.G. Fierro (Eds.), Stud. Surf. Sci. Catal., vol. 130, Elsevier, Amsterdam, 2000, p. 197.
[8] I. Rossetti, L. Forni, Appl. Catal., B: Environ. 33 (2001) 345.
[9] G.L. Chiarello, I. Rossetti, L. Forni, J. Catal. 236 (2005) 251.
[10] A. Abragam, B. Bleaney, Electron Paramagnetic Resonance of Transition Ions, Oxford University Press, New York, 1970.
[11] J.M. Baker, in: G.R. Eaton, S.S. Eaton, K.M. Salikhov (Eds.), Foundations of Modern EPR, World Scientific, Singapore, 1998 (Chapter B.3).
[12] D.M. Bagguley, B. Bleaney, Contemp. Phys. 31 (1990) 35.
[13] B. Bleaney, Proc. R. Soc. Lond. A 433 (1991) 461.
[14] A.I. Shames, E. Rozenberg, V. Markovich, M.I. Auslender, A. Yakubovsky, A. Maignan, C. Martin, B. Raveau, G. Gorodetsky, Solid State Commun. 126 (2003) 395.
[15] J. Smit, J. Appl. Phys. 37 (1966) 1455.
[16] E.L. Nagaev, Physics of Magnetic Semiconductors, MIR, Moscow, 1983.
[17] A. Barman, M. Ghosh, S. Biewas, S.K. De, S. Chatterjee, Appl. Phys. Lett. 71 (1997) 3150.
[18] P. Aleshkevych, M. Baran, S.N. Barilo, J. Fink-Finowicki, H. Szymczak, J. Phys: Condens. Matter 16 (2004) L179.
[19] T.L. Phan, M.H. Phan, N.V. Khiem, N.X. Phuc, S.C. Yu, J. Magn. Magn. Mater. 282 (2004) 299.
[20] C. Oliva, L. Forni, A.V. Vishniakov, Spectrochim. Acta A 56 (2000) 301.